Journal of Materials Chemistry C

Dynamic Article Links ▶

ARTICLE

Direct observation of the work function evolution of graphene-two dimensional metal contacts

Songbo Yang †, Peng Zhou†*, Lin Chen†, Qingqing Sun†*, Pengfei Wang†, Shijin Ding†, Anquan Jiang† and David Wei Zhang†

The work function evolution of graphene monolayer under two dimensional metal electrodes was studied by combining in-situ metal deposition and ultraviolet photoelectron spectroscopy under an ultra-high vacuum system. The process of the charge transfer at the graphene-metal interfaces was investigated. The transfer of electrons from metal to graphene and then from graphene to metal, with the
10 metal deposition, was observed. The work function of the graphene-metal contact shifted, and finally was pinned at the theoretical work function of metal when the metal turned from a two dimensional film into a bulk material. Meanwhile, the energy barrier of the metal/graphene interface could be tailored by metal thickness freely. It brought much possibility to put forward the graphene device application.

15

Introduction

The work function of contact metal in a graphene-metal contact is critical in the high performance of graphene spin-electronic and high-frequency electronic devices [1-2], such as
20 the carrier mobility and static current properties. The interaction and charge transfer processes between graphene and a bulk metal contact have recently been evaluated using the first-principle calculation [2-4]. However, there are few experimental investigations on the work function evolution of graphene under
25 metal films and charge transfer at the interfaces, especially at the graphene/ultra-thin metal interfaces, which play a key role in the performance of graphene-based electronic devices. Indirect scanning kelvin probe microscopy (SKPM) [5-7] and current-voltage (C-V) methods [8-11] have been used to study the work
30 function of graphene-metal contact interfaces with low sensitivity and low reliability. Direct measurements of graphene-two dimensional metal contact interfaces and the charge transfer dynamic processes have not been investigated in detail and are essential in the application of graphene devices [8].
35 In this report, the work function of nickel (Ni) and titanium (Ti) with different thicknesses, ranging from two dimensional to bulk, on graphene and the interfacial charge transfer processes were directly observed with ultraviolet photoelectron spectroscopy (UPS) in an in-situ ultra-high vacuum system. The
40 two dimensional metal was deposited on graphene, resulting in deposited metal-graphene interfaces, in contrast to graphene on the metal substrate.[12, 13] In the initial interfacial charge transfer dynamic process, electrons moved from two dimensional metal to the graphene film. As a result, a few dipoles were
45 formed at the interface. However, the direction of the transferred electrons began to change with increasing thickness of metal. Meanwhile, the energy barrier of metal/graphene also changed

with different metal thicknesses, which contributed to forming good ohmic contacts and reducing the contact resistances in the
50 future graphene devices.

Experimental

The fabrication of monolayer graphene was carried out by chemical vapour deposition as described in Supporting materials
55 S1 section. The monolayer graphene was measured by Raman spectroscopy and then loaded into the multi-functional surface analysis system.
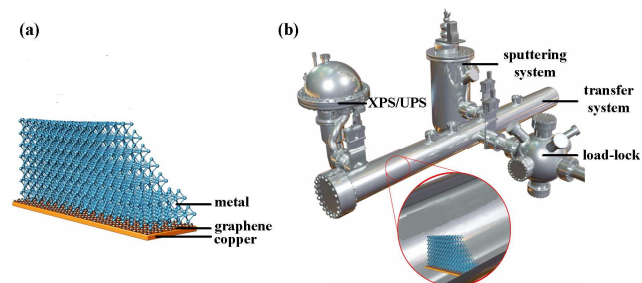
Figure 1. The experiment of graphene-metal contacts was made with the in-situ system. Three-dimensional diagrams of (a)
60 *different thicknesses of metal deposited on graphene and (b) the multi-functional surface analysis system.*

Fig. 1 shows a diagram of experimental design. The monolayer thick graphene sample was transferred into the load-lock and
65 measured initially in an X-ray photoelectron spectroscopy-ultraviolet photoelectron spectroscopy (XPS/UPS) chamber with a pressure of 8.0×10^{-10} mbar. Then metal films (nickel and titanium) with different thicknesses were deposited on graphene by an in-situ magnetron sputtering system as shown in Fig. 1(a)
70 and Fig. 1(b). The graphene film could be restored by treating it

at 300 °C for 60 minutes. The original valance band energy level and the work function of the pristine graphene were recorded by XPS/UPS. The sample was subsequently transferred into the sputtering chamber. The sample was transferred back into the XPS/UPS chamber and UPS spectroscopy was applied to analyse the energy band structure after depositing metal in sputtering system. This process was repeated from 0.2nm until the thickness of the metal film reached 4.2 nm.

Results and discussion
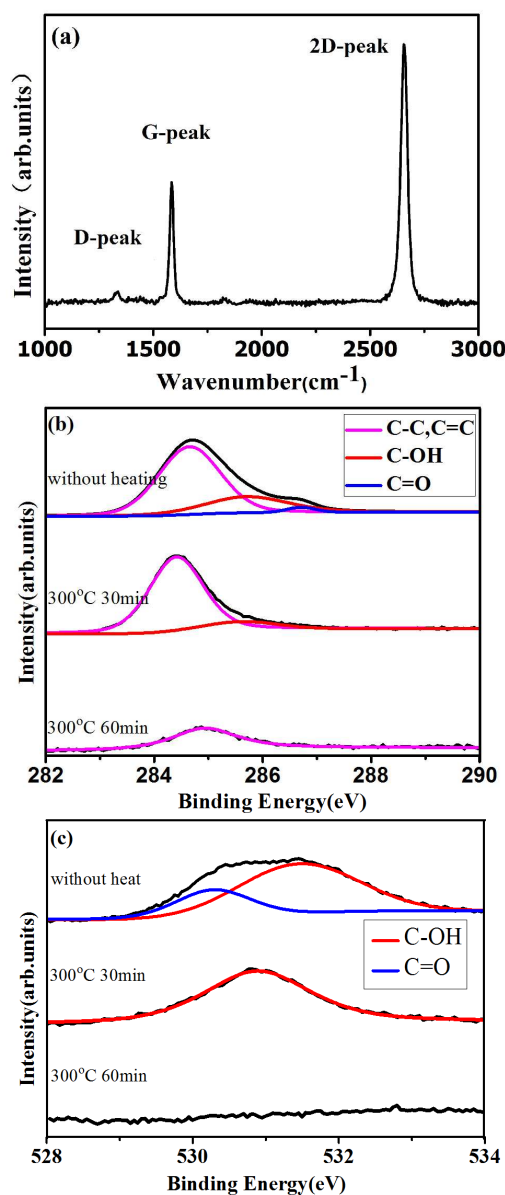
Figure 2. The characterization of graphene before graphene-metal contacts forming. (a) Raman spectrum of graphene as fabricated. (b) and (c) show C_{1s} and O_{1s} peaks with different thermal heating minutes, respectively. It is obvious the high quality graphene is achieved after 300 °C thermal treatment for 60 minutes in high vacuum.
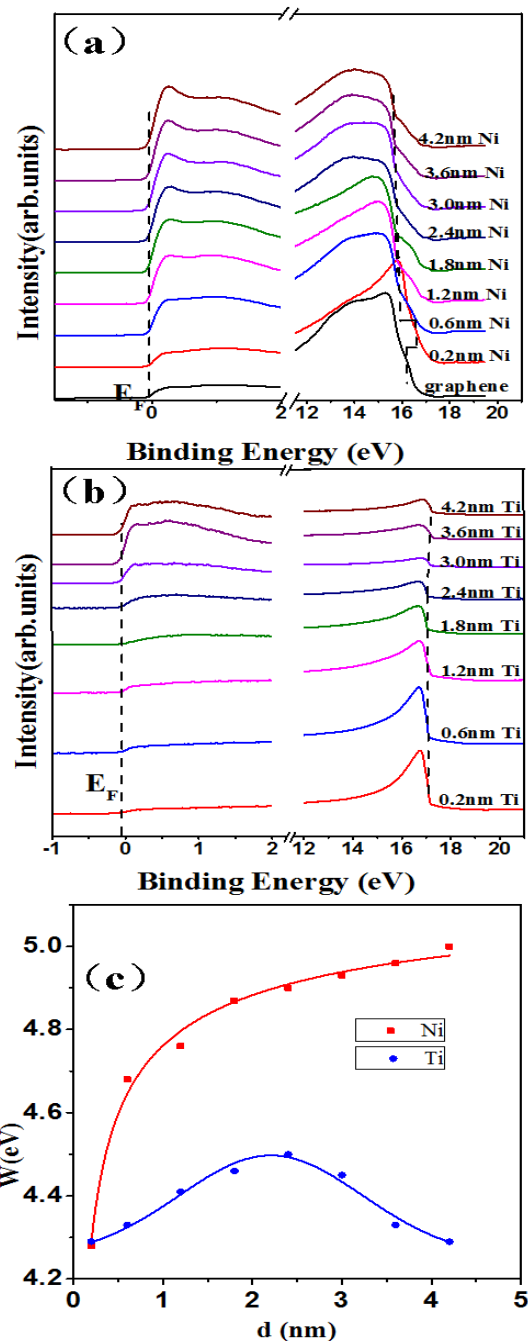
Figure 3. The work function evolution of metal-graphene contact with the metal dimension varying. UPS spectra of the (a) graphene-nickel and (b) graphene-titanium interface as a function of the thickness of metal contact that was deposited on graphene. (c) The work function of the graphene-metal interface as a function of the thickness of the metal contact overlayer.

Raman spectroscopy of graphene on SiO_2/Si substrate was carried out with a 514 nm laser, as shown in Fig. 2(a). The I_{2D}/I_G ratio value was 2.2，and it confirmed that the graphene film was the monolayer. A low disorder-induced D band (~1338 cm^{-1}) was also observed. In order to achieve high quality graphene, thermal

treatment in high vacuum condition was applied. The effects of thermal treatments were shown in Fig. 2(b) for C_{1s} and Fig. 2(c) for O_{1s}, respectively. C_{1s} peaks of graphene as fabricated could be separated into C−C, C=C, C−OH and C=O function groups (Fig.

[5] 2(b)), which were located at binding energies of 284.6, 285.6 and 286.7 eV, respectively.[14-16] The C=O and C−OH functional groups of the O_{1s} peak (Fig. 2(c)) corresponded to binding energies of 530.3 and 531.5 eV, respectively.[16] After a 300 °C treatment was carried out for 30 minutes, the C=O peak

[10] disappeared. After heating for 60 minutes, only the C−C and C=C peaks were observed. Analysis of the O1s peak supports the information obtained by analysis of the C_{1s} in Fig. 2(c). After the thermal treatment for 30 minutes, the C−OH group was missing and the intensity had decreased. From the O_{1s} spectrum of the

[15] sample treated at 300 °C for 60 minutes, oxygen was not present. This is consistent with the results from the C_{1s} peaks. Finally, the number of defects in the graphene was reduced and the quality of the graphene was improved.

Fig. 3 (a) and (b) display images of the UPS spectra for

[20] different thicknesses of nickel and titanium on graphene, respectively, where the thickness ranged from two dimensional to bulk. In this study, the UPS spectra were measured with He I radiation (hυ = 21.22 eV, where hυ is the energy of the photons). The resolution was 0.13 eV. The sample was characterized with a

[25] negative bias (−8 V) to compensate for the contact potential between the sample and the detector.[17-18] The work function (W) is determined by the following equation: W = hυ − (E$_{cutoff}$ − E$_{Fermi}$), where E$_{cutoff}$ and E$_{Fermi}$ are the binding energies of the secondary electron cutoff and the Fermi level, respectively. [19-

[30] 20] According to Fig. 3(a) and Fig. 3(b), the work function of fresh graphene, measured by using UPS, was 4.55 ± 0.13 eV (W = hυ − (E$_{cutoff}$ − E$_{Fermi}$) = 21.22 − (16.50 − 0.03) = 4.55 eV). [21] With the UPS spectra and the equation of work function, the metal work functions were calculated with different thicknesses

[35] of metal films, as shown in Fig. 3(c).

An important phenomenon was observed where the work function increased from 4.28 eV (21.22−(16.97−0.03)= 4.28 eV) to 5.00 eV (21.22−(16.25−0.03)= 5.00 eV) at the graphene-Ni interface, and went up from 4.29 eV (21.22−(16.96−0.03)=

[40] 4.29eV) to 4.50 eV (21.22−(16.75−0.03)= 4.50 eV) and then down to 4.29 eV at the graphene-Ti interface when the metal thickness gradually increased from 0.2 nm to 4.2 nm, as shown in Fig. 3(c).When the thickness of the metal was below 2 nm, it could be regarded as a sort of two dimensional metal. Hence, the

[45] work function shift could be understood as the charge transfer and energy level alignment at the graphene-metal interface.

This phenomenon is illustrated in Fig. 4(a)-(f). The work function of 0.2 nm two dimensional nickel was 4.28eV (W = hυ − (E$_{cutoff}$ − E$_{Fermi}$) = 21.22 − (16.97 − 0.03) = 4.28 eV), which was

[50] directly measured by UPS, was smaller than the work function of fresh graphene (4.55 eV). When 0.2 nm nickel was deposited on the surface of graphene and graphene-nickel interfaces were formed, Fermi levels of both metal and graphene would be coupled. As the Fermi level in two dimensional nickel was higher

[55] than in graphene, electrons moved from two dimensional nickel to graphene. In the course of transferring electrons, the Fermi level of graphene shifted upward with respect to the Dirac point, finally it was the same with nickel Fermi level, as shown in Fig.

4(a). Thus at the initial stage electrons shifted from two

[60] dimensional metal to graphene.
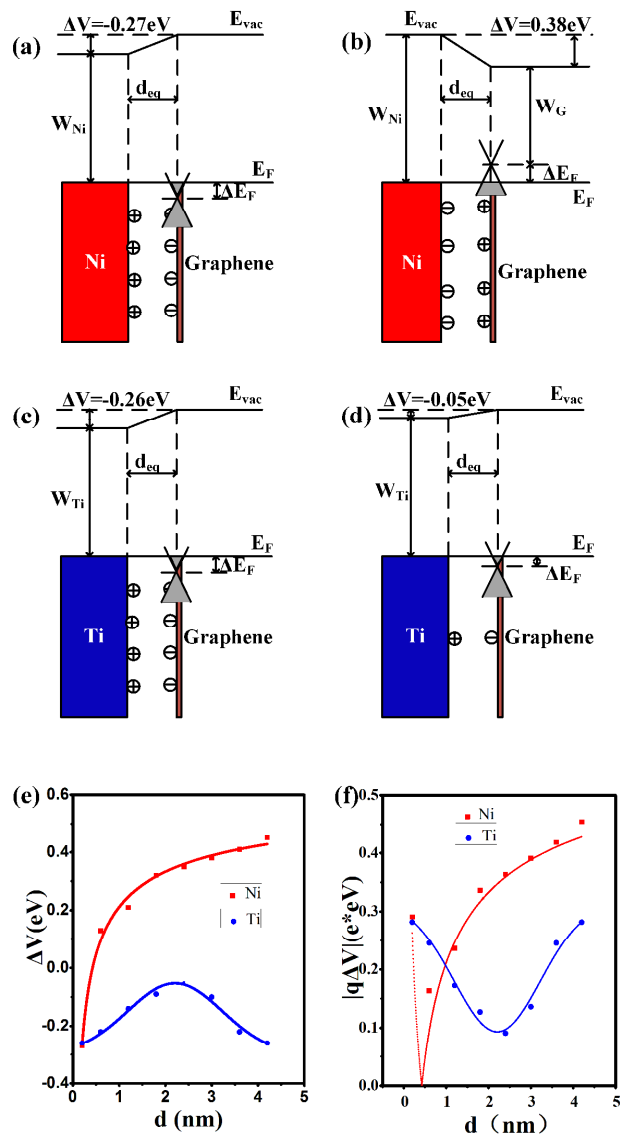
Figure 4. *The analysis of metal-graphene contact as to two dimensional and bulk metal. Interfacial energy diagrams of (a) 0.2 nm and (b) 3.0 nm thick nickel, (c) 0.2 nm and (d) 2.4 nm*
[65] *thick titanium overlayers on graphene at the graphene-metal interface. (e) The difference in the work function between metal and graphene (ΔV) as a function of the thickness of the metal overlayer. (f)The energy barrier of metal/graphene (|qΔV |) as a function of the thickness of the metal. The vacuum energy level*
[70] *(E$_{vac}$), ΔV, the equilibrium interfacial distance (d$_{eq}$), the Fermi level (E$_F$), the difference in the energy levels between the Dirac point and Fermi level of graphene (ΔE$_F$), the work function of nickel (W$_{Ni}$), the work function of nickel (W$_{Ti}$), the work function of graphene (W$_G$) and the thickness of the metal overlayer (d) are*
[75] *shown in Fig 4(a)–(f).*

When the two dimensional nickel was increasing from 0.2 nm to 3.0 nm, the measured work function of interface rose, as shown in Fig. 3 (c), which caused a new alignment process in energy

levels of both sides of interfaces. Therefore, electrons, which were accumulated in graphene before, began to leave. The direction of charge transfer had changed and graphene became less and less n-doped by electrons. Thus the Fermi level of graphene gradually shifted downward to couple with nickel. After the energy level alignment in 3.0-nm-thick bulk nickel, as shown in Fig. 4(b), the ΔV arrived 0.38 eV (4.93-4.55=0.38 eV). Compared with the Fig. 4(a), the direction of the electric field formed by interfacial dipoles turned into the opposite direction. It is important that we observed the electron transport direction began to change with increasing nickel contact thickness for the first time.

As the theoretical work function of titanium is 4.33 eV, which is smaller than the value for intrinsic graphene (4.55 eV) and is regarded as a reference to the nickel. It was also found that the direction of charge transfer had changed with increasing titanium film thickness, as shown in Fig. 4(c) - Fig. 4(f). When the titanium film was two dimensional, it was almost the same with nickel for charge transfer at interfaces. In Fig. 4(c), 0.2-nm-thick two dimensional titanium on graphene lead to electrons moved from titanium to graphene and graphene became n-doped. When the titanium thickness gradually increased from 0.2 nm to 2.4 nm, the work function of the graphene-Ti interface increased from 4.29 eV to 4.50 eV, as shown in Fig. 3(c). Meanwhile, the energy level alignment occurred at interfaces. A part of electrons in graphene began to move back to titanium, which contributed that graphene was less n-doped. The Fermi energy level also went down, but it was still higher than its Dirac point. The geometry of metal contact began to change from two dimensional to bulk when the thickness of metal from 2.4nm to 4.2 nm. The work function of bulk titanium-graphene interface did not increased with the thickness, it began to decrease and finally was pinned at 4.26 eV (21.22− (16.99−0.03) = 4.26 eV), regardless of the thickness of the contact, which was consistent with the theoretical value for titanium (4.33 eV). Meanwhile, electrons began to accumulate in graphene again, as a result, the Fermi level of graphene-titanium interface gradually rose. Finally, the work function of titanium, measured by UPS, tended to the theoretical value of titanium.

Therefore, the conclusion could be drawn that electrons first moved from metal to graphene when 0.2-nm-thick two dimensional metal was on fresh graphene, then the direction of charge transfer changed and some electrons left from graphene. Meanwhile, the work function of the graphene-metal contact shifted, with the metal deposition, was pinned at the theoretical work function of metal when the metal turned into a bulk material.

During the process of depositing metal films, electrons shifted and the potential barrier was formed at the interfaces. The energy barrier of metal/graphene changed with increasing metal thickness, as shown in Fig. 4(f). The curves of the energy barrier displayed with "V" shape. With the certain metal thickness, the energy barrier could arrive the minimum. The minimum value in nickel was smaller than in titanium, meaning that nickel is good for graphene contacts. Graphene devices, with such Ni/Au (~0.5/30 nm) and Ti/Au (~2.4/30 nm) contacts, were fabricated to verify the mechanism and did prove that there are some improvements in the contact resistivity and Ni/Au contacts are much better than Ti/Au contacts for graphene devices. Thus the energy barrier of metal/graphene can be tuned by metal thickness actually. It brings much possibility to put forward the graphene based device application by tailoring the metal-graphene contact barrier freely.

Conclusions

In summary, the work function evolution at graphene-metal interfaces and the charge transfer process were precisely determined using in-situ metal deposition and UPS measurements. During this process, the direction of the charge transfer changed and the work function of the graphene-metal interface first increased and finally was pinned at the theoretical work function of metal when the thickness of metal increased from 0.2 to 4.2 nm. Meanwhile, the energy barrier of metal/graphene could be tuned by the deposited metal thickness. This work helped to further understanding in the mechanism of the graphene-metal interface and form good ohmic contacts. It also contributed in the understanding of how to form a high quality graphene electrode, which is promising for future graphene electronic devices.

Notes and references

a Address, †ASIC & System State Key Lab, School of Microelectronics, Fudan University, Shanghai 200433, China
correspondence to pengzhou@fudan.edu.cn, qqsun@fudan.edu.cn

† Electronic Supplementary Information (ESI) available: [Supporting Information is available from the authors.]. See DOI: 10.1039/b000000x/

[1] B. J. Schultz, C. Jaye, P. S. Lysaght, D. A. Fischer, D. Prendergast, and S. Banerjee, Chemical Science 4 (1), 494 (2013).
[2] P. A. Khomyakov, G. Giovannetti, P. C. Rusu, G. Brocks, J. van den Brink, and P. J. Kelly, Physical Review B 79 (19), 195425 (2009).
[3] C. Gong, G. Lee, B. Shan, E. M. Vogel, R. M. Wallace, and K. Cho, Journal of Applied Physics 108 (12), 123711 (2010).
[4] R. Mao, B. D. Kong, C. Gong, S. Xu, T. Jayasekera, K. Cho, and K. W. Kim, Physical Review B 87 (16), 165410 (2013).
[5] D. Ziegler, P. Gava, J. Güttinger, F. Molitor, L. Wirtz, M. Lazzeri, A. M. Saitta, A. Stemmer, F. Mauri, and C. Stampfer, Physical Review B 83 (23), 235434 (2011).
[6] W. J. Liu, H. Y. Yu, S. H. Xu, Q. Zhang, X. Zou, J. L. Wang, K. L. Pey, J. Wei, H. L. Zhu, and M. F. Li, Electron Device Letters, IEEE 32 (2), 128 (2011).
[7] Y. Yu, Y. Zhao, S. Ryu, L. E. Brus, K. S. Kim, and P. Kim, Nano Letters 9 (10), 3430 (2009).
[8] Y. Lin, X. Li, D. Xie, T. Feng, Y. Chen, R. Song, H. Tian, T. Ren, M. Zhong, and K. Wang, Energy & Environmental Science 6 (1), 108 (2013).
[9] Y. Murata, E. Starodub, B. B. Kappes, C. V. Ciobanu, N. C. Bartelt, K. F. McCarty, and S. Kodambaka, Applied Physics Letters 97 (14), 143113 (2010).
[10] M. S. Choi, S. H. Lee and W. J. Yoo, Journal of Applied Physics 110 (7), 73305 (2011).

[11] J. Park, W. H. Lee, S. Huh, S. H. Sim, S. B. Kim, K. Cho, B. H. Hong, and K. S. Kim, The Journal of Physical Chemistry Letters 2 (8), 841 (2011).

5   [12] Lahiri, J.; Batzill, M. Graphene Destruction by Metal Carbide Formation: An Approach for Patterning of Metal-Supported Graphene.Appl. Phys. Lett.2010, 97,023102.

[13] Gong, C.; McDonnell, S.; Qin, X.; Azcatl, A.; Dong, H.; Chabal, Y. J.; Cho, K.; Wallace, R. M., Realistic Metal–Graphene Contact Structures. ACS Nano 2013, 8, (1), 642-649.

10   [14] S. Yumitori, Journal of materials science 35 (1), 139 (2000).

[15] D. Yang, A. Velamakanni, G. Bozoklu, S. Park, M. Stoller, R. D. Piner, S. Stankovich, I. Jung, D. A. Field, and C. A. Ventrice Jr, Carbon 47 (1), 145 (2009).

[16] A. Pirkle, J. Chan, A. Venugopal, D. Hinojos, C. W. Magnuson, S.
15   McDonnell, L. Colombo, E. M. Vogel, R. S. Ruoff, and R. M. Wallace, Applied Physics Letters 99 (12), 122103 (2011).

[17] S. T. Lee, X. Y. Hou, M. G. Mason, and C. W. Tang, Applied Physics Letters 72 (13), 1593 (1998).

[18] I. G. Hill and A. Kahn, Journal of applied physics 84 (10), 5583
20   (1998).

[19] W. Song and M. Yoshitake, Applied Surface Science 251 (1), 14 (2005).

[20] Y. Park, V. Choong, Y. Gao, B. R. Hsieh, and C. W. Tang, Applied Physics Letters 68 (19), 2699 (1996).

25   [21] C. Gong, D. Hinojos, W. Wang, N. Nijem, B. Shan, R. M. Wallace, K. Cho, and Y. J. Chabal, ACS Nano 6 (6), 5381 (2012).

30

35